Dioxomolybdenum(VI)-Modified Mesoporous MCM-41 and MCM-48 Materials for the Catalytic Epoxidation of Olefins

Carla D. Nunes,[a] Martyn Pillinger,[a] Anabela A. Valente,[a] João Rocha,[a] André D. Lopes,[b] and Isabel S. Gonçalves*[a]

Keywords: Molybdenum / N ligands / Mesoporous materials / Supported catalysts / Epoxidations

The dioxomolybdenum(VI) complex $[MoO_2Cl_2(L\text{-}L)]$, containing the bidentate 1,4-diazabutadiene ligand RN=C(Ph)–C(Ph)=NR [R = $(CH_2)_3Si(OEt)_3$], was immobilised in the ordered mesoporous silica MCM-41 by carrying out a grafting reaction in dichloromethane. The grafted material (3.3 wt.-% Mo) was tested as a catalyst for the epoxidation of cyclooctene with *tert*-butyl hydroperoxide (TBHP) at 55 °C. Selectivity to the epoxide was very high and the observed kinetic profile was similar to that of the complex $[MoO_2Cl_2(L\text{-}L)]$ in the homogeneous phase. On recycling several times, some activity was lost from the first to second runs, but thereafter stabilised. Tethered complexes of this type were also prepared by a stepwise approach. The mesoporous silicas MCM-41 and MCM-48 were first treated with a toluene solution of the ligand L-L under reflux. Before isolating the grafted materials, the silylating agent Me_3SiCl was added to remove the residual Si–OH groups on the surface of the mesoporous materials. Oxomolybdenum species were subsequently introduced into the ligand-silicas by pore volume impregnation of a solution of the complex $[MoO_2Cl_2(THF)_2]$ in CH_2Cl_2 at room temperature. The modified materials have been characterised by powder X-ray diffraction, N_2 adsorption, and solid-state MAS NMR (^{13}C, ^{29}Si). Despite having lower metal loadings (1 wt.-% Mo), the materials exhibited similar catalytic activities for the epoxidation of cyclooctene to that of the modified MCM-41 with 3.3 wt.-% of Mo. However, selectivities to the epoxide were lower. The MCM supported catalysts have also been tested for the epoxidation of cyclododecene and α-pinene with TBHP.

Introduction

High-valent d^0 transition metal complexes, such as Mo^{VI}, V^V, and Ti^{IV}, are effective catalysts for the selective epoxidation of olefins by alkyl hydroperoxides (ROOH).[1] In particular, Mo^{VI} complexes of the type $[MoO(O_2)_2(L^1)(L^2)]$ and $[MoO_2X_2(L^1)(L^2)]$ (X = Cl, Br, CH_3), with different combinations of base ligands L^1 and L^2, have been experimentally characterised and tested as catalysts for epoxidation reactions, usually employing *tert*-butyl hydroperoxide (TBHP) as the mono-oxygen source.[2,3] It is ever more accepted that alkyl peroxides activate these complexes by an intermediate η^2-coordination of the peroxidic agent to the Lewis acidic metal centre.[4] Important properties, such as the solubility of the complex and the Lewis acidity of the metal centre, can be fine-tuned by variation of either X or L.

Despite the good results obtained for oxomolybdenum(VI) complexes in homogeneous catalysis, increasing attention is being paid to heterogeneous catalysts since these can be easily separated from a reaction mixture and recycled, which is of significant industrial interest. The immobilisation of transition metal catalysts, for example on an inorganic support,[5] may also eliminate other problems associated with homogeneous catalysis, such as dimerisation of the active complex or auto-oxidation. One approach is to use support materials modified with Lewis base ligands. Sherrington and co-workers reported that polymer-supported molybdenum(VI) complexes are active and recyclable catalysts for olefin epoxidation with TBHP.[6] For inorganic supports, a general strategy is to use functional alkoxy silanes. Corma et al. have prepared dioxomolybdenum(VI) complexes with chiral ligands derived from (2*S*,4*R*)-4-hydroxyproline.[7] The complexes bearing a $Si(OEt)_3$ group were heterogenised to a modified USY-zeolite by covalent bonding.

Micelle-templated silicas as catalyst supports for transition metal catalysts have been extensively studied over the last decade,[5] and are often more effective than amorphous silica.[8] This is probably due to the unique combination of a high surface area, allowing a good dispersion of active sites, with an ordered mesoporous structure, allowing selective catalysis in a constrained environment. Jia and Thiel modified the ordered mesoporous silica MCM-41 with a bidentate pyrazolylpyridine ligand and prepared a coval-

[a] Department of Chemistry, CICECO, University of Aveiro, Campus de Santiago, 3810-193 Aveiro, Portugal
Fax: (internat.) +351-234-370084
E-mail: igoncalves@dq.ua.pt
[b] Faculty of Science and Technology, Department of Chemistry and Biochemistry, University of the Algarve, Campus de Gambelas, 8000-062 Faro, Portugal

  DOI: 10.1002/ejic.200300278

ently anchored complex of the type $[MoO(O_2)_2(L\text{-}L)]$.[9] The hybrid system was highly active and truly heterogeneous for liquid-phase epoxidation of cyclooctene with TBHP as the oxygen source. The molybdenum(VI) complexes $[MoO_2Cl_2(L^1)(L^2)]$ have also been immobilised in MCM-41 derivatised with monodentate nitrile and bidentate bipyridyl ligands.[10] Unfortunately, they are unstable towards molybdenum leaching, which accounts for their nearly complete loss of activity in a second reaction cycle. The high molybdenum loadings resulted in weakly adsorbed Mo dimeric species that were easily extracted during the oxidative transformations.

In the present work, we have attempted to prepare more stable heterogeneous olefin epoxidation catalysts by immobilisation of dioxomolybdenum(VI) complexes in the ordered mesoporous silicas MCM-41 and MCM-48 functionalised with a bidentate 1,4-diazabutadiene ligand.

Results and Discussion

The supported catalysts were prepared from MCM-41 and MCM-48 materials (Scheme 1). First, the triethoxysilyl ligand RN=C(Ph)−C(Ph)=NR (**1**) [R = $(CH_2)_3Si(OEt)_3$] was prepared by the reaction of benzil $[C_6H_5(CO)(CO)C_6H_5]$ with two equivalents of (3-aminopropyl)triethoxysilane. Treatment of the solvent adduct $[MoO_2Cl_2(THF)_2]$ with one equivalent of the ligand **1** gave the complex $[MoO_2Cl_2(L\text{-}L)]$ (**2**) in good yield. Such complexes, with bidentate substituted 1,4-diazabutadiene ligands L-L (RN=CR′−CR′=NR), are active, stable homogeneous catalysts for the epoxidation of olefins using TBHP.[3b] Treatment of MCM-41 with a solution of complex **2** in dichloromethane gave a modified material **3** containing approximately 3.3 wt.-% Mo (0.34 mmol·g^{-1}). The solid-state ^{13}C CP MAS NMR spectrum of **3** was similar to that of **2** except for less intense peaks corresponding to the OEt groups (δ = 58.4 and 18.3), due to the grafting on MCM-41. Tethered complexes of this type were also prepared by an alternative stepwise approach. MCM-41 and MCM-48 were first treated with a toluene solution of **1** under reflux. Before isolating the grafted materials, the silylating agent Me_3SiCl was added to remove the residual Si−OH groups on the surface of the mesoporous materials, which could be unfavourable for the catalytic reaction.[9] Trimethylsilylation may also render the surface more hydrophobic and improve stability against moisture and mechanical compression. Oxomolybdenum species were subsequently introduced into the ligand-silicas **4** (MCM-41) and **6** (MCM-48) by pore volume impregnation of a solution of the dioxomolybdenum(VI) complex $[MoO_2Cl_2(THF)_2]$ in CH_2Cl_2 at room temperature. Elemental analysis indicated metal loadings of 1.0 wt.-% (0.10 mmol·g^{-1}) for **5** (MCM-41) and 1.4 wt.-% (0.14 mmol·g^{-1}) for **7** (MCM-48).

The solid-state ^{13}C CP MAS NMR spectra of the ligand-silicas **4** and **6**, and the derivatised materials **5** and **7**, were similar to those of the grafted material **3**, confirming the presence of surface-bound 1,4-diazabutadiene groups. An

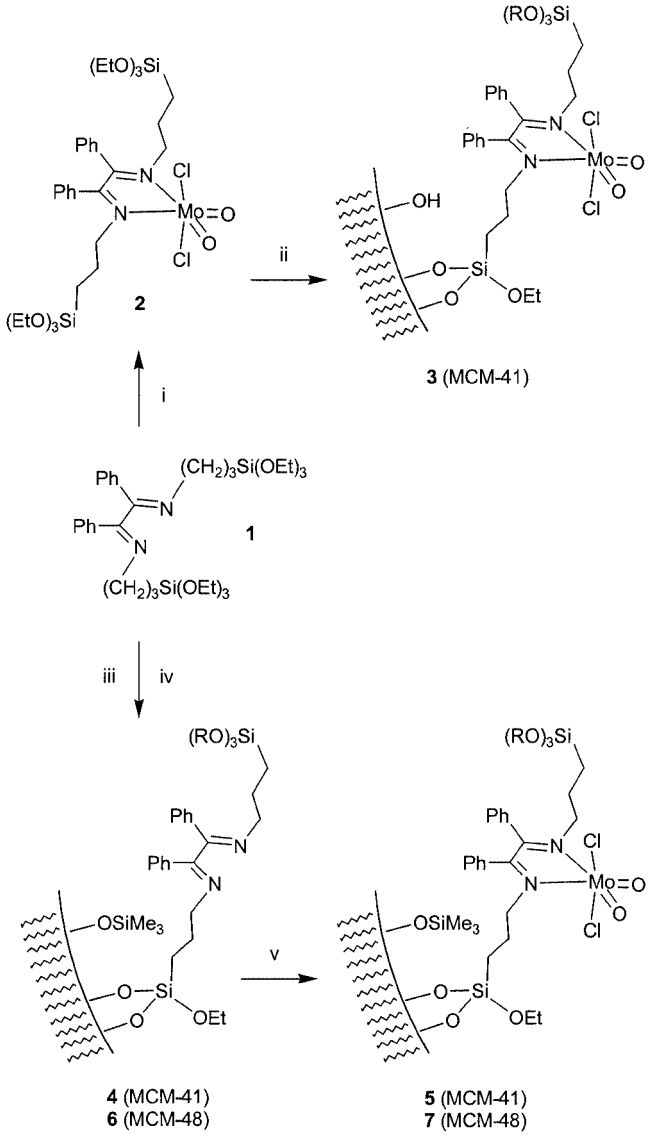

Scheme 1. Reagents: i, THF, $[MoO_2Cl_2(THF)_2]$; ii, CH_2Cl_2, MCM-41; iii, toluene, MCM-41 or MCM-48; iv, Me_3SiCl; v, CH_2Cl_2, $[MoO_2Cl_2(THF)_2]$

additional peak at about δ = −0.5 was attributed to $(-O)_3Si-O-SiMe_3$ species. The solid-state ^{29}Si MAS NMR spectra of the grafted materials **3**−**7** provide direct evidence for the incorporation of the covalently anchored organic system. Figure 1 shows the ^{29}Si MAS and CP MAS NMR spectra for pristine calcined MCM-41, the ligand-silica **4**, and the derivatised material **5**. Similar results were obtained for the corresponding MCM-48 materials. Unmodified MCM-41 displays two broad convoluted resonances in the ^{29}Si CP MAS NMR spectrum at δ = −110.7 and −100.9, assigned to Q^4 and Q^3 species of the silica framework, respectively [$Q^n = Si(OSi)_n(OH)_{4-n}$]. A weak shoulder is also observed at δ = −91.0 for the Q^2 species. The Q^3 sites are associated with the single silanols Si−OH (including hydrogen-bonded silanols), and the Q^2 sites correspond to the geminal silanols. Grafting of the triethoxysilane ligand **1** and Me_3SiCl into MCM-41 reduces

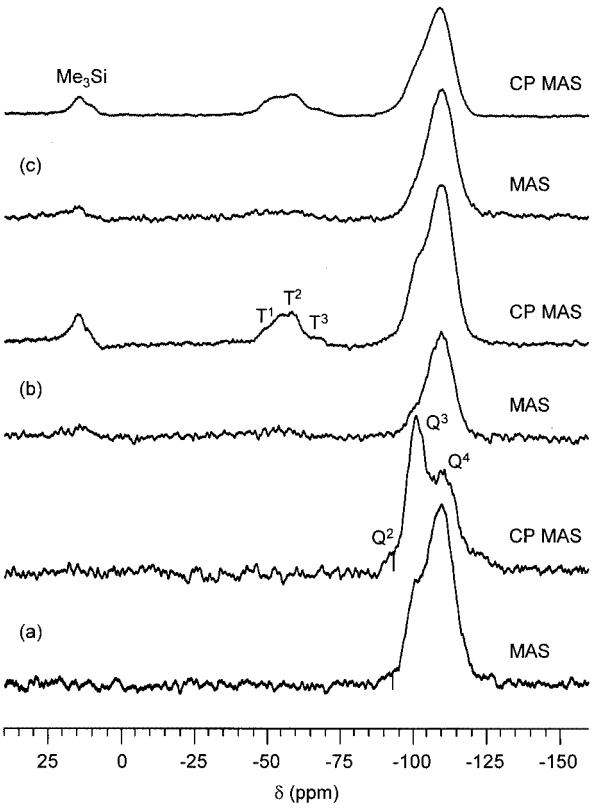

Figure 1. ^{29}Si MAS and CP MAS NMR spectra of (a) MCM-41, (b) MCM-41-L/Me_3SiCl (**4**), and (c) MCM-41-L/Me_3SiCl/MoO_2Cl_2 (**5**)

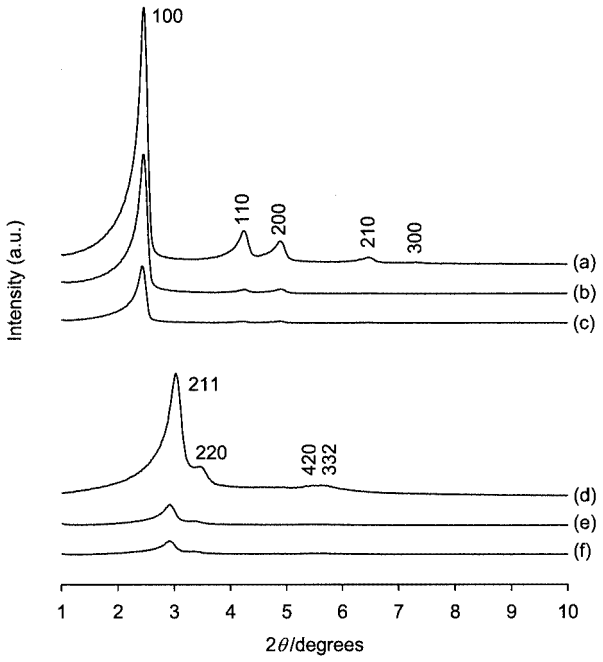

Figure 2. Powder XRD patterns of (a) MCM-41, (b) MCM-41-L/Me_3SiCl (**4**), (c) MCM-41-L/Me_3SiCl/MoO_2Cl_2 (**5**), (d) MCM-48, (e) MCM-48-L/Me_3SiCl (**6**), and (f) MCM-48-L/Me_3SiCl/MoO_2Cl_2 (**7**)

the Q^3 and Q^2 resonances and, concomitantly, increases the Q^4 resonance. This is consistent with esterification of the isolated silanol groups by nucleophilic substitution at the silicon atom in the organic compounds. The ^{29}Si CP MAS NMR spectrum of **4** reveals unchanged Q^3 silicon atoms. These might be hydrogen-bonded surface silanols, $(SiO)_3Si-OH-OH-Si(SiO)_3$, which are unreactive to silylating agents.[11] The ^{29}Si CP MAS NMR spectra of **4** and **6** also display two signals at $\delta = -50.0$ and -58.5, assigned to T^1 and T^2 organosilica species, respectively [$T^m = R.Si(OSi)_m(OEt)_{3-m}$]. A weak, broad signal at $\delta = -67.5$ is assigned to a T^3 environment, and a sharp peak at about $\delta = 14.0$ to the silicon nuclei of the Me_3Si groups. Reaction of the ligand-silicas **4** and **6** with the complex $[MoO_2Cl_2(THF)_2]$ does not measurably change the ^{29}Si MAS and CP MAS NMR spectra (Figure 1).

The powder XRD patterns of the pristine calcined MCM-41 and MCM-48 starting materials agree with reported patterns, indicating well-ordered materials (Figure 2).[12,13] Several distinct Bragg peaks are observed in the range $2\theta = 2-8°$, which can be indexed to different *hkl* reflections. MCM-41 is indexed on a hexagonal unit cell (using the strongest reflection, d_{100}, $a = 2d_{100}/\sqrt{3} = 41.4$ Å) and MCM-48 on a cubic unit cell (using the strongest reflection, d_{211}, $a = d_{211}\sqrt{6} = 71.5$ Å). Upon grafting with the triethoxysilyl ligand **1** and Me_3SiCl, several distinct Bragg peaks are still observed, indicating retention of the long-range hexagonal and cubic symmetries (Figure 2). A significant attenuation of the XRD peak intensities is not interpreted as a loss of order, but to a likely reduction in the X-ray scattering contrast between the silica walls and pore-filling material.[14] Reaction of the ligand-silicas **4** and **6** with the complex $[MoO_2Cl_2(THF)_2]$ does not change the powder XRD patterns significantly. There is a further slight reduction of peak intensities, for the reason outlined above. A similar result was obtained after reaction of the complex $[MoO_2Cl_2(THF)_2]$ with MCM-41 functionalised with bipyridyl groups.[10b]

The pristine MCM solids show reversible type IV N_2 adsorption−desorption isotherms, typical of mesoporous solids (pore width between 2 and 50 nm, according to IUPAC).[15] The step corresponding to capillary condensation in the primary mesopores appears in the relative pressure ranges 0.3−0.4 and 0.15−0.27 for unmodified MCM-41 and MCM-48, respectively, and is less pronounced for the latter (Figure 3). The specific surface area and total pore volume of the pristine MCM materials are greater than 940 $m^2 \cdot g^{-1}$ and 0.7 $cm^3 \cdot g^{-1}$, respectively (Table 1). The isotherms of the functionalised MCM samples show a lower N_2 uptake, pointing to a decrease in the specific surface area and pore volume. This effect is more pronounced for the trimethylsilylated samples **5** and **7**, for which S_{BET} decreased more than 33% and V_p decreased more than 56%. The height of the capillary condensation step and the p/p_0 coordinate of the inflection point decreases significantly, indicating changes in pore size distribution due to grafting of the internal silica surface with the molybdenum species and, for **5** and **7**, with Me_3SiCl.[10b,16,17] This is confirmed by comparing the pore size distributions (PSD) of the pristine and modified MCM materials (Figure 3). Upon surface

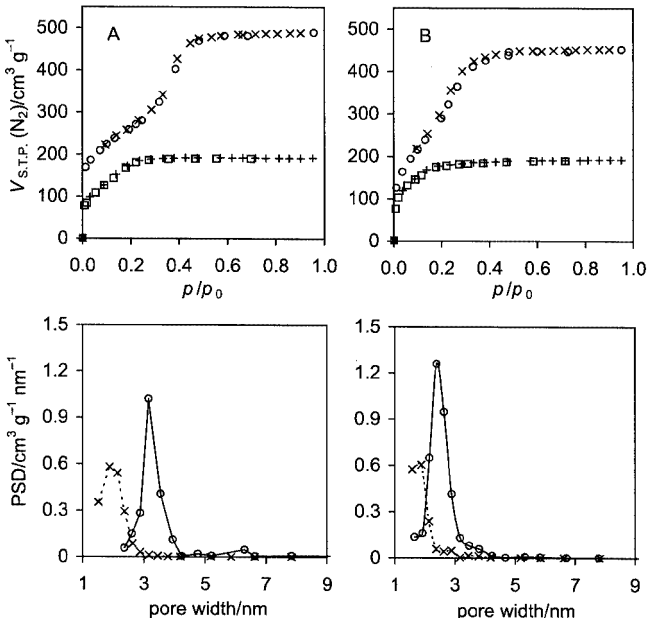

Figure 3. Nitrogen isotherms at 77 K of pristine MCM-41 (A) and MCM-48 (B) [(O) adsorption; (×) desorption], and surface-grafted **5** (A) and **7** (B) [(□) adsorption; (+) desorption]. Pore size distribution curves are also shown for the pristine (—) and surface-grafted materials (- - -)

grafting, the PSDs shift towards smaller pore sizes and the peaks become lower, indicating decreased uniformity of the pores.

The catalytic performance of complex **2** was studied for the epoxidation of cyclooctene with TBHP at 55 °C (1% molar ratio of complex/cyclooctene). After one hour the turnover frequency (TOF) was 18 mmol g^{-1}_{cat} h^{-1} and after 24 h the selectivity to cyclooctene oxide was 96% at 56% conversion (Table 2). The activity of **2** is similar to that reported under identical reaction conditions for other (dichloro)dioxomolybdenum(VI) catalysts bearing 1,4-diazabutadiene ligands without aromatic substituents.[3b] Despite using excess of oxidant with respect to the substrate, cyclooctene conversion at 24 h is still far from quantitative. In these catalysts the molybdenum centre acts as a Lewis acid, thereby decreasing the electron density in the coordinated TBHP molecule and promoting nucleophilic attack of the olefin on the O−O bond.[4b] The formation of *tert*-butyl alcohol during epoxidation may contribute to the decay in the reaction rate since it may act as a competitive inhibitor for the attack of TBHP at the Mo centre.[4b,10a,18] Conversely, although the complex bears relatively stable chelating nitrogen ligands,[3b,3c] the pendant triethoxysilyl groups may furnish less reactive dimers/oligomers, thus accounting for catalyst deactivation during epoxidation.

As described above, complex **2** was grafted onto the surface of MCM-41 to give the supported catalyst **3** at a metal loading of approximately 3.3 wt.-% Mo. The catalytic results obtained in the presence of **3** are similar to those obtained in homogeneous phase for complex **2** (Table 2, Figure 4). The corresponding kinetic curves are alike, suggesting a similar reaction mechanism. The reaction rate decreases after 7 h reaching a maximum conversion of 65% after 24 h (Table 2). Such retardation may result from the competitive reaction of the active Mo complex with *tert*-butyl alcohol, as in the homogeneous phase, and/or catalyst deactivation. The stability of catalyst **3** was studied by reusing the recovered solid in three consecutive reaction cycles. Before each reuse the solid was separated from the reaction solution, thoroughly washed with dichloromethane and dried at 60 °C. The catalytic activity decreased from the first to the second run, but afterwards tended to remain constant (Table 2, Figure 4). Probably, weakly adsorbed molybdenum complexes that were not efficiently solvent extracted after the grafting reaction were leached to the reaction solution. The catalyst stability was further investigated by reusing **3** in a fourth reaction cycle. After 2 h, the catalyst was separated at the reaction temperature and the solution was stirred for another 4 h. Cyclooctene conversion remained practically unchanged and molybdenum was not detected in the reaction solution by ICP-AES. Furthermore, the FTIR spectra of the solids recorded before and after catalysis showed no major changes. These results suggest that catalyst **3** is fairly stable and that catalysis is, in principle, heterogeneous.

The modified materials **5** and **7** were also tested as catalysts for the epoxidation of cyclooctene with TBHP at 55 °C. Considering the initial activities, the epoxidation of cyclooctene in the presence of **5** is slightly faster than for **7** (TOF = 6.7 and 5.9 mmol·g^{-1}_{cat}·h^{-1}, respectively), despite the lower molybdenum content of the former. However, at 24 h, both catalysts give approximately 63% conversion (Table 2). Overall, the kinetic profiles for **5** and **7** are similar (Figure 5). The difference in initial activities may be due, in part, to different internal diffusion rates during the initial unsteady operation as a result of the different channel structures of the mesoporous hosts. MCM-41 consists of an

Table 1. Texture parameters of MCM samples taken from nitrogen adsorption data

Sample	S_{BET} [$m^2 \cdot g^{-1}$]	ΔS_{BET} (%)[a]	V_P [$cm^3 \cdot g^{-1}$]	ΔV_P (%)[b]	d_p [nm]
MCM-41−1	1033	−	0.78	−	3.5
3	803	−22	0.56	−28	3.2
MCM-41−2	948	−	0.76	−	3.2
5	630	−34	0.30	−61	1.9
MCM-48−1	1161	−	0.70	−	2.4
7	672	−42	0.30	−57	1.9

[a] Variation of surface area in relation to parent MCM material. [b] Variation of total pore volume in relation to parent MCM material.

Table 2. Catalytic results of cyclooctene epoxidation with catalysts **2**, **3**, **5**, or **7**, at 55 °C

Catalyst	TOF [mmol·g$^{-1}_{cat}$·h^{-1}][a]	Conversion (%)[b]	Selectivity to cyclooctene oxide (%)[c]
2	18	56	96
3 (run, 1)	4.5	65	100
3 (run, 2)	0.7	50	98
3 (run, 3)	0.4	48	98
5 (run, 1)	6.7	62	81
5 (run, 2)	1.1	55	89
5 (run, 3)	0.7	50	92
7 (run, 1)	5.9	63	94
7 (run, 2)	0.8	58	94
7 (run, 3)	0.5	55	95

[a] Calculated for ca. 1 hour reaction. [b] Cyclooctene conversion after 24 h. [c] 1,2-Cyclooctanediol was formed.

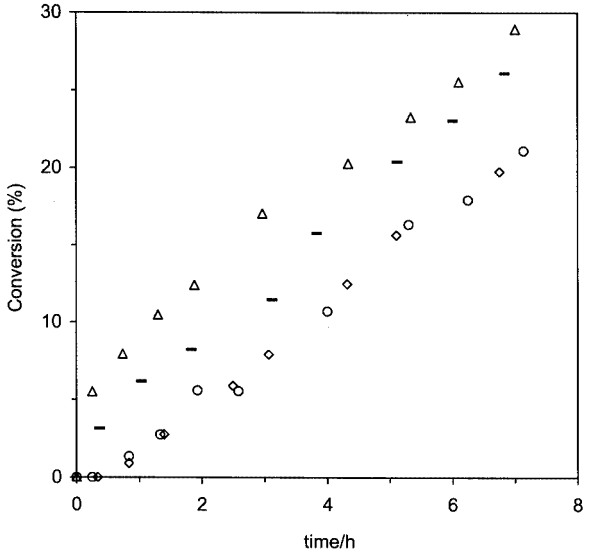

Figure 4. Kinetic profiles of cyclooctene epoxidation in the presence of **2** (−) and **3** [(Δ) − run 1; (O) − run 2; (◇) − run 3]

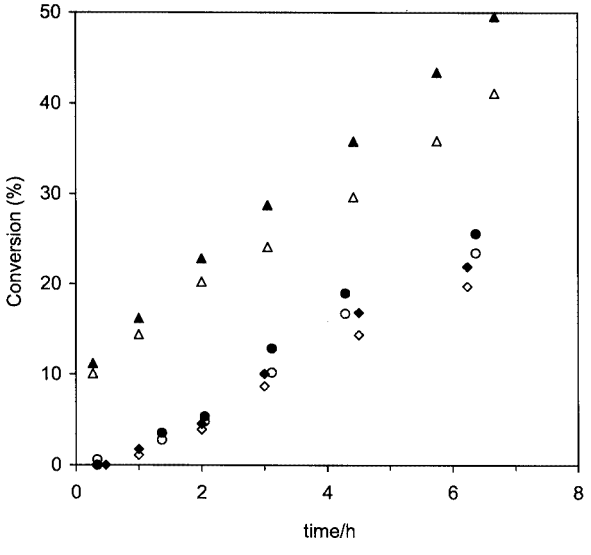

Figure 5. Kinetic profiles of cyclooctene epoxidation in the presence of **5** [(▲) − run 1; (●) − run 2; (◆) − run 3] and **7** [(Δ) − run 1; (O) − run 2; (◇) − run 3]

hexagonal arrangement of cylindrical pores, whereas MCM-48 possesses a three-dimensional gyroid-type pore structure. Despite the lower Mo loadings of catalysts **5** and **7** in comparison to **3**, they are more active initially (Table 2). Trimethylsilyation of MCM-41 and MCM-48 makes the surface more hydrophobic, thereby enhancing the adsorption of the olefin, and concomitantly reducing the adsorption of polar *tert*-butyl alcohol, making the Mo centres more available for the attack of TBHP. For catalysts **5** and **7** the selectivity to cyclooctene oxide is lower than for **3** and the complex **2**. This is unexpected since the adsorption of the polar epoxide should be less favourable on a more hydrophobic surface. Probably, trace amounts of HCl, which remained inside the MCM materials after silylation, are responsible for the ring opening reaction. In fact, selectivity to 1,2-cyclooctanediol decreases in recycling runs (Table 2). The stability of **5** and **7** was studied in a similar fashion to that of **3**. The Mo loading after three reaction cycles is at least 99% of the original value, as ascertained by ICP-AES. The main loss of catalytic activity is observed from the first to the second run, but the activity then tends to remain constant, similar to that observed for **3** (Table 2, Figure 4). The leaching of some weakly adsorbed molybdenum complexes present in the fresh catalyst may account for the initial loss of activity.

The MCM catalysts **3**, **5**, and **7** were also tested for the epoxidation of cyclododecene and α-pinene with TBHP at 55 °C (Figure 6). For each catalyst, olefin conversion at 24 h decreases in the order: cyclooctene (Cy8=) > cyclododecene (Cy12=) > α-pinene. Cyclododecene oxidation yields exclusively the corresponding epoxide (Cy12 oxide). A higher conversion is achieved with **3** (60% at 24 h) than with **5** and **7**, which may be due to the faster diffusion of the bulky substrate molecules inside the wider pores of **3**. For α-pinene oxidation, less than 2.5% α-pinene oxide is yielded at 24 h. The main reaction product is campholenic aldehyde (< 6% yield), which is an intermediate for sandalwood fragrance santalol and may be formed by the Lewis acid catalysed rearrangement of α-pinene oxide.[18,19]

Conclusions

The prepared supported catalysts reported here are active for the epoxidation of olefins using TBHP as the oxidant.

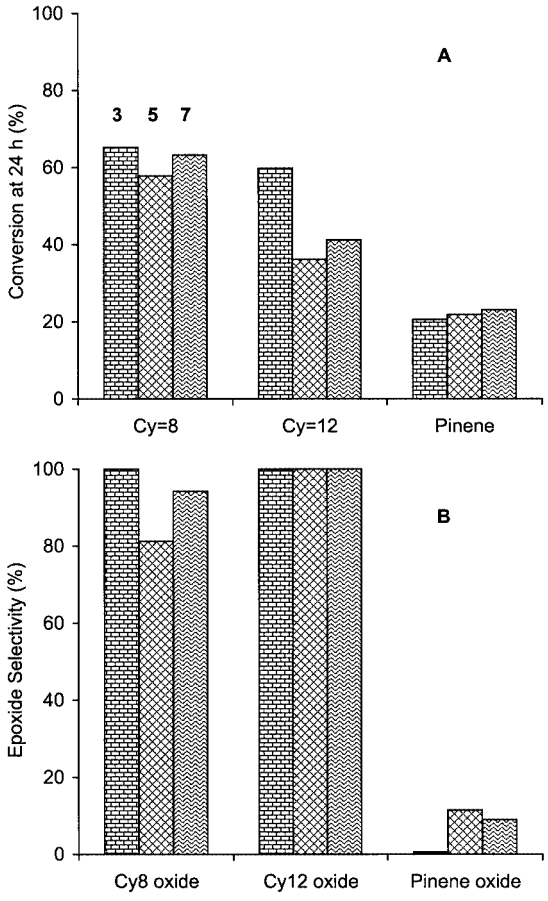

Figure 6. Conversion of cyclooctene (Cy8=), cyclododecene (Cy12=) and α-pinene (A) and selectivity towards the epoxide (B) observed for **3** (bricks), **5** (diamonds) or **7** (waves), at 24 h

Some activity is lost from the first to second runs, but thereafter the solids can be recycled without significant loss of activity. Tests indicate that the recycled solids operate as true heterogeneous catalysts. Previously, 2,2′-bipyridine was covalently grafted to MCM-41 and the resulting MoO_2Cl_2 supported material used as an epoxidation catalyst.[10b] However, most of the observed activity was due to leached molybdenum species in solution. Better results have been obtained here by using the 1,4-diazabutadiene ligand bearing triethoxysilyl groups. Future studies will centre on the use of this chelating ligand to immobilise other transition metal homogeneous catalysts.

Experimental Section

Material and Methods: Starting materials were obtained from commercial sources and used as received. All preparations and manipulations were carried out using standard Schlenk techniques under nitrogen. Solvents were dried by standard procedures (THF, hexane, and diethyl ether with Na/benzophenone ketyl; CH_2Cl_2 with CaH_2), distilled under nitrogen and kept over 4 Å molecular sieves. The solvent adduct $[MoO_2Cl_2(THF)_2]$ was prepared as described previously.[20]

Microanalyses were performed at the University of Aveiro. Powder XRD data were collected on a Phillips X'pert diffractometer using Cu-K_α radiation filtered by Ni. Nitrogen adsorption−desorption isotherms were measured at 77 K, using a gravimetric adsorption apparatus equipped with a CI electronic MK2−M5 microbalance and an Edwards Barocel pressure sensor. Before the measurements the MCM silicas were outgassed at 450 °C and the modified materials at 140 °C (to minimise destruction of the functionalities) and maintained at that temperature overnight to a residual pressure of ca. 10^{-4} mbar. The texture parameters, BET specific surface area (S_{BET}) and specific total pore volume (micropore plus mesopore, V_P), were estimated from the adsorption isotherm data. The pore size distribution curves (PSD − differential volume adsorbed with respect to the differential pore size per unit mass vs. pore width) were computed from the desorption branch of the experimental isotherms, using a method based on the area of the pore walls.[15,21] Assuming open cylindrical pores with radius r_p and zero contact angle and correcting for the thickness of the layer already adsorbed, r_p can be calculated by summing the Kelvin radius and the statistical average thickness (t, calculated using the Halsey equation) of the adsorbed layer.

IR spectra in transmission mode were measured with a Mattson Mod 7000 FTIR spectrometer using KBr pellets. Raman spectra were recorded on a Bruker RFS 100/S FT Raman spectrometer using a 1064 nm excitation of the Nd/YAG laser. ^1H and ^{13}C solution NMR spectra were obtained with a Bruker AMX-300 spectrometer. ^{29}Si and ^{13}C solid-state NMR spectra were recorded at 79.49 and 100.62 MHz, respectively, on a (9.4 T) Bruker Avance 400P spectrometer. ^{29}Si MAS NMR spectra were recorded with 40° pulses, spinning rates 5.0−5.5 kHz, and 60 s recycle delays. ^{29}Si CP MAS NMR spectra were recorded with 5.5 μs ^1H 90° pulses, 8 ms contact time, a spinning rate of 4.5 kHz, and 4 s recycle delays. ^{13}C CP MAS NMR spectra were recorded with a 4.5 μs ^1H 90° pulse, 2 ms contact time, a spinning rate of 8 kHz, and 4 s recycle delays. Chemical shifts are quoted in ppm from TMS. ^{13}C spectra were also recorded in the solid state at 125.76 MHz on a Bruker Avance 500 spectrometer.

MCM-41 and MCM-48: Purely siliceous MCM-41 was synthesised as described previously using $[(C_{14}H_{29})N(CH_3)_3]Br$ ($C_{14}TMABr$) as the templating agent.[10b] MCM-48 was crystallised from a gel with the molar composition SiO_2:0.26Na_2O:60H_2O:0.8$C_{16}TMABr$. Specifically, a solution of tetraethyl orthosilicate (17.36 g, 0.083 mol) in H_2O (30 mL) was added slowly to a vigorously stirred solution of $[(C_{16}H_{33})N(CH_3)_3]Br$ (24.05 g, 0.066 mol) in H_2O (40 mL). A solution of NaOH (1.76 g, 0.044 mol) in water (20 mL) was then added and the resulting mixture was stirred for 30 min and then autoclaved at 110 °C for 2 days in Teflon-lined stainless steel reaction vessels. The solid product was recovered by filtration, washed with hot water and air-dried at 30 °C. Calcination at 540 °C for 6 h then removed the surfactant template. Before the grafting experiments with MCM-41 and MCM-48, physisorbed water was removed from the calcined materials by heating at 180 °C in vacuo (10^{-2} Pa) for 2 h.

Ph-DAB-$(CH_2)_3Si(OEt)_3$ (1): A solution of (3-aminopropyl)triethoxysilane (2.85 g, 12.9 mmol) in THF (10 mL) was added to a solution of benzil (1.35 g, 6.4 mmol) in THF, followed by 4 Å molecular sieves (1.6 mm pellets, 0.6 g) and a catalytic amount of $ZnCl_2$. After 12 h at 50 °C the solution was filtered , and the resultant residue rinsed with THF and the filtrate evaporated in vacuo to give the product as a pale yellow oil (3.98 g) in 84.7% yield. IR (KBr): $\tilde{\nu}$ = 3062 (m), 2973 (vs), 2926 (vs), 2885 (vs), 1674 (vs), 1626 (s), 1595 (s), 1579 (s), 1448 (s), 1390 (s), 1318 (m), 1294 (m), 1281 (m), 1220 (s), 1166 (vs), 1102 (vs), 1062 (vs), 957 (vs), 792 (s), 776 (s), 724 (m), 696 (s), 623 (m) cm^{-1}. ^1H NMR (300.13 MHz,

$CDCl_3$, 25 °C, TMS): δ = 0.60−0.68 (m, 4 H, $SiCH_2$), 1.15−1.24 (m, 18 H, OCH_2CH_3), 1.76−1.86 (m, 4 H, $CH_2CH_2CH_2$), 3.40−3.44 (t, 4 H, NCH_2), 3.73−3.84 (m, 12 H, OCH_2CH_3), 7.32−7.50 (m, 5 H, Ph), 7.57−7.75 (m, 3 H, Ph), 7.88−7.93 (m, 2 H, Ph) ppm. $^{13}C\{^1H\}$ NMR (75.47 MHz, $CDCl_3$, 25 °C, TMS): δ = 8.0 ($SiCH_2$), 18.3 (OCH_2CH_3), 24.3 ($CH_2CH_2CH_2$), 56.4 (CH_2N=C), 58.1 (OCH_2CH_3), 127.2, 128.6, 129.1 (Ph), 166.3 (CH_2N=*C*) ppm. ^{29}Si NMR (59.62 MHz, $CDCl_3$, 25 °C, TMS): δ = −52.90 ppm. $C_{32}H_{52}N_2O_6Si_2$ (616.99): calcd. C 62.30, H 8.50, N 4.54; found C 62.00, H 8.41, N 4.28.

MoO_2Cl_2[Ph-DAB-$(CH_2)_3Si(OEt)_3$] (2): A solution of $MoO_2Cl_2(THF)_2$ (0.25 g, 0.75 mmol) in THF (10 mL) was treated with 1 equivalent of the ligand **1** in THF (5 mL). The resulting turbid solution was stirred for a further 30 min at room temperature. The solvent was then evaporated, and the resultant solid product washed with hexane and dried in vacuo. Yield: 0.47 g, 76%. IR (KBr): $\tilde{\nu}$ = 2973 (s), 1681 (s), 1674 (vs), 1594 (s), 1491 (m), 1449 (s), 1306 (m), 1230 (m), 1077 (vs), 1047 (vs), 984 (s), 943 (vs), 915 (vs), 879 (s), 774 (m), 703 (m), 684 (m), 643 (m) cm^{-1}. ^{13}C CP MAS NMR: δ = 9.6 ($SiCH_2$), 18.3 (OCH_2CH_3), 21.7 ($CH_2CH_2CH_2$), 55.0 (CH_2N=C), 58.4 (OCH_2CH_3), 128.8 (Ph), 167.5 (CH_2N=*C*) ppm. ^{29}Si MAS NMR: δ = −54.4 ppm. $C_{32}H_{52}Cl_2MoN_2O_8Si_2$ (816.90): calcd. C 46.99, H 6.65, N 3.42; found C 46.56, H 6.29, N 3.38.

MCM-41/MoO_2Cl_2[Ph-DAB-$(CH_2)_3Si(OEt)_3$] (3): A solution of **2** (0.40 g, 0.49 mmol) in CH_2Cl_2 (10 mL) was added to a suspension of MCM-41 (1.0 g) in CH_2Cl_2 (15 mL) and the mixture stirred at room temperature for 24 h. The solution was then filtered and the so-obtained pale blue powder washed repeatedly with CH_2Cl_2 (4 × 20 mL), before drying in vacuo at room temperature for several hours. IR (KBr): $\tilde{\nu}$ = 1633 (m), 1596 (w), 1450 (m), 1384 (w), 1230 (sh), 1078 (vs), 954 (m), 914 (sh), 798 (m), 568 (m), 455 (s) cm^{-1}. ^{13}C CP MAS NMR: δ = 8.7, 15.6, 21.1, 53.2, 58.8, 128.7, 131.7, 136.6, 137.9 ppm. ^{29}Si MAS NMR: δ = −50.4, −56.2, −102.6 (Q^3), −108.0 (Q^4) ppm. Elemental analysis found C 8.50, N 0.49, H 0.90, Mo 3.3.

MCM-41-L/Me_3SiCl (4): A solution of the ligand **1** (0.66 g, 1.07 mmol) in toluene (5 mL) was added to a suspension of MCM-41 (1.0 g) in toluene (10 mL) and the mixture heated at 100 °C for 9 h. After cooling to ambient temperature, Me_3SiCl (5 mL) was added and the mixture stirred at room temperature for a further 24 h. The resultant solid was then filtered off and washed twice with acetone (2 × 20 mL), twice with CH_2Cl_2 (2 × 15 mL), and dried in vacuo at 100 °C for 3 h. Selected FT Raman: $\tilde{\nu}$ = 3069 (m), 2961 (m), 2904 (s), 1600 (s), 1552 (w), 1452 (m), 1415 (w), 1028 (w), 1001 (s), 617 (m) cm^{-1}. ^{13}C CP MAS NMR: δ = −0.5 (Me_3SiO−), 8.4 ($SiCH_2$), 16.4, 20.8, 24.9, 57.8, 127.6 (phenyl-C) ppm. ^{29}Si MAS NMR: δ = 14.5 (bd), −53.8 (bd), −109.5 ppm. ^{29}Si CP MAS NMR: δ = 13.8 (Me_3SiO−), −54.0 (T^1), −58.5 (T^2), −67.5 (T^3), −102.0 (sh, Q^3), −108.8 (sh, Q^4) ppm. Elemental analysis found C 16.24, N 1.34, H 2.33.

MCM-41-L/Me_3SiCl/MoO_2Cl_2 (5): A solution of $MoO_2Cl_2(THF)_2$ (0.52 g, 1.5 mmol) in CH_2Cl_2 (5 mL) was added to a suspension of the ligand-silica **4** (1.0 g) in CH_2Cl_2 (10 mL) and the mixture stirred overnight at room temperature. The resultant solid was then filtered off and washed with CH_2Cl_2 (4 × 20 mL), and dried in vacuo at room temperature for 3 h. Selected FT Raman: $\tilde{\nu}$ = 3069 (m), 2962 (m), 2904 (s), 1602 (m), 1001 (m) cm^{-1}. ^{13}C CP MAS NMR: δ = −0.3 (Me_3SiO−), 9.3 ($SiCH_2$), 20.8, 25.0, 57.9, 128.5 (phenyl-C). ^{29}Si MAS NMR: δ = 14.6, −55.0 (bd), −110.0 ppm. ^{29}Si CP MAS NMR: δ = 14.4 (Me_3SiO−), −54.0 (T^1), −58.0 (T^2), −67.5 (T^3), −108.9 (sh, Q^4) ppm. Elemental analysis found C 10.94, N 1.25, H 2.63, Mo 1.0.

MCM-48-L/Me_3SiCl (6): A solution of the ligand **1** (0.71 g, 1.15 mmol) in toluene (5 mL) was added to a suspension of MCM-48 (1.15 g) in toluene (10 mL) and the mixture heated at 100 °C for 9 h. After cooling to ambient temperature, Me_3SiCl (5 mL) was added and the mixture stirred at room temperature for a further 24 h. The so-obtained solid was then filtered off and washed twice with acetone (2 × 20 mL), twice with CH_2Cl_2 (2 × 15 mL), and dried in vacuo at 100 °C for 3 h. Selected FT Raman: $\tilde{\nu}$ = 3068 (s), 2971 (m), 2932 (s), 2901 (s), 1599 (s), 1550 (w), 1452 (m), 1414 (w), 1028 (w), 1001 (s), 617 (m) cm^{-1}. ^{13}C CP MAS NMR: δ = −0.3 (Me_3SiO−), 9.3 ($SiCH_2$), 17.0, 20.8, 58.9, 128.2 (phenyl-C) ppm. ^{29}Si MAS NMR: δ = −109.6 ppm. ^{29}Si CP MAS NMR: δ = 13.9 (Me_3SiO−), −50.0 (T^1), −58.4 (T^2), −67.5 (T^3), −101.9 (Q^3), −109.4 (Q^4) ppm. Elemental analysis found C 13.38, N 1.30, H 2.33.

MCM-48-L/Me_3SiCl/MoO_2Cl_2 (7): A solution of $MoO_2Cl_2(THF)_2$ (0.52 g, 1.5 mmol) in CH_2Cl_2 (5 mL) was added to a suspension of the ligand-silica **6** (1.0 g) in CH_2Cl_2 (10 mL) and the mixture stirred overnight at room temperature. The resultant solid was then filtered off and washed with CH_2Cl_2 (4 × 20 mL), and dried in vacuo at room temperature for 3 h. Selected FT Raman: $\tilde{\nu}$ = 3066 (m), 2962 (m), 2903 (s), 1598 (m), 1001 (m) cm^{-1}. ^{13}C CP MAS NMR: δ = 0.7 (Me_3SiO−), 8.7 ($SiCH_2$), 17.5, 20.7, 58.9, 128.7 (phenyl-C), 184.4 ppm. ^{29}Si MAS NMR: δ = 14.8, −55.0 (bd), −108.7 ppm. ^{29}Si CP MAS NMR: δ = 14.7 (Me_3SiO−), −54.7 (T^1), −59.4 (T^2), −67.5 (T^3), −108.7 (Q^4) ppm. Elemental analysis found C 10.94, N 1.30, H 2.63, Mo 1.4.

Catalysis: The liquid-phase epoxidation of cyclooctene was carried out at 55 °C under air in a micro reaction vessel equipped with a magnetic stirrer, which was loaded with complex (0.073 mmol) or MCM-catalyst (175 mg), olefin (7.3 mmol) and TBHP (11 mmol, 5.5 M in decane). Samples were withdrawn periodically and analysed using a gas chromatograph (Varian 3800) equipped with a capillary column (SPB-5, 20 m × 0.25 mm × 0.25 μm) and a flame ionisation detector. Undecane was used as internal standard added after the reaction.

Acknowledgments

The authors are grateful to FCT, POCTI, and FEDER for financial support (Project PCTI/1999/QUI/32889). CN thanks the University of Aveiro and the FCT for research grants. Paula Brandão and Cláudia Morais are acknowledged for assistance with the NMR experiments.

[1] [1a] K. A. Jörgensen, *Chem. Rev.* **1989**, *89*, 431−458. [1b] M. H. Dickman, M. T. Pope, *Chem. Rev.* **1994**, *94*, 569−584. [1c] C. C. Romão, F. E. Kühn, W. A. Herrmann, *Chem. Rev.* **1997**, *97*, 3197−3246. [1d] A. Corma, H. García, *Chem. Rev.* **2002**, *102*, 3837−3892.

[2] [2a] W. R. Thiel, M. Angstl, T. Priermeier, *Chem. Ber.* **1994**, *127*, 2373−2379. [2b] W. R. Thiel, M. Angstl, N. Hansen, *J. Mol. Catal. A: Chem.* **1995**, *103*, 5−10. [2c] W. R. Thiel, T. Priermeier, *Angew. Chem. Int. Ed. Engl.* **1995**, *34*, 1737−1738. [2d] W. R. Thiel, J. Eppinger, *Chem. Eur. J.* **1997**, *3*, 696−705.

[3] [3a] F. E. Kühn, E. Herdtweck, J. J. Haider, W. A. Herrmann, I. S. Gonçalves, A. D. Lopes, C. C. Romão, *J. Organomet. Chem.* **1999**, *583*, 3−10. [3b] F. E. Kühn, A. D. Lopes, A. M. Santos, E. Herdtweck, J. J. Haider, C. C. Romão, A. G. Santos, *J. Mol. Catal. A: Chem.* **2000**, *151*, 147−160. [3c] F. E. Kühn,

A. M. Santos, A. D. Lopes, I. S. Gonçalves, E. Herdtweck, C. C. Romão, *J. Mol. Catal. A: Chem.* **2000**, *164*, 25−38.

[4] [4a] A. Hroch, G. Gemmecker, W. R. Thiel, *Eur. J. Inorg. Chem.* **2000**, 1107−1114, and references cited therein. [4b] F. E. Kühn, M. Groarke, É. Bencze, E. Herdtweck, A. Prazeres, A. M. Santos, M. J. Calhorda, C. C. Romão, I. S. Gonçalves, A. D. Lopes, M. Pillinger, *Chem. Eur. J.* **2002**, *8*, 2370−2383, and references cited therein.

[5] D. E. De Vos, M. Dams, B. F. Sels, P. A. Jacobs, *Chem. Rev.* **2002**, *102*, 3615−3640.

[6] [6a] D. C. Sherrington, *Catal. Today* **2000**, *57*, 87−104. [6b] S. Leinonen, D. C. Sherrington, A. Sneddon, D. McLoughlin, J. Corker, C. Canevali, F. Morazzoni, J. Reedijk, S. B. D. Spratt, *J. Catal.* **1999**, *183*, 251−266. [6c] M. M. Miller, D. C. Sherrington, *J. Catal.* **1995**, *152*, 368−376. [6d] M. M. Miller, D. C. Sherrington, *J. Catal.* **1995**, *152*, 377−383.

[7] A. Corma, A. Fuerte, M. Iglesias, F. Sánchez, *J. Mol. Catal. A: Chem.* **1996**, *107*, 225−234.

[8] [8a] J. Jarupatrakorn, J. D. Tilley, *J. Am. Chem. Soc.* **2002**, *124*, 8380−8388. [8b] R. D. Oldroyd, G. Sankar, J. M. Thomas, D. Ozkaya, *J. Phys. Chem. B* **1998**, *102*, 1849−1855. [8c] A. Maldotti, A. Molinari, G. Varani, M. Lenarda, L. Storaro, F. Bigi, R. Maggi, A. Mazzacani, G. Sartori, *J. Catal.* **2002**, *209*, 210−216.

[9] [9a] M. Jia, W. R. Thiel, *Chem. Commun.* **2002**, 2392−2393. [9b] M. Jia, A. Seifert, W. R. Thiel, *Chem. Mater.* **2003**, *15*, 2174−2180.

[10] [10a] P. Ferreira, I. S. Gonçalves, F. E. Kühn, A. D. Lopes, M. A. Martins, M. Pillinger, A. Pina, J. Rocha, C. C. Romão, A. M. Santos, T. M. Santos, A. A. Valente, *Eur. J. Inorg. Chem.* **2000**, 2263−2270. [10b] C. D. Nunes, A. A. Valente, M. Pillinger, A. C. Fernandes, C. C. Romão, J. Rocha, I. S. Gonçalves, *J. Mater. Chem.* **2002**, *12*, 1735−1742.

[11] X. S. Zhao, G. Q. Lu, A. K. Whittaker, G. J. Miller, H. Y. Zhu, *J. Phys. Chem. B* **1997**, *101*, 6525−6531.

[12] [12a] C. T. Kresge, M. E. Leonowicz, W. J. Roth, J. C. Vartuli, J. S. Beck, *Nature* **1992**, *359*, 710−712. [12b] J. S. Beck, J. C. Vartuli, W. J. Roth, M. E. Leonowicz, C. T. Kresge, K. D. Schmitt, C. T. -W. Chu, D. H. Olson, E. W. Sheppard, S. B. McCullen, J. B. Higgins, J. L. Schlenker, *J. Am. Chem. Soc.* **1992**, *114*, 10834−10843.

[13] [13a] A. A. Romero, M. D. Alba, W. Zhou, J. Klinowski, *J. Phys. Chem. B* **1997**, *101*, 5294−5300. [13b] J. Xu, Z. Luan, H. He, W. Zhou, L. Kevan, *Chem. Mater.* **1998**, *10*, 3690−3698.

[14] [14a] B. Marler, U. Oberhagemann, S. Vortmann, H. Gies, *Microporous Mater.* **1996**, *6*, 375−383. [14b] W. Hammond, E. Prouzet, S. D. Mahanti, T. J. Pinnavaia, *Micropor. Mesopor. Mater.* **1999**, *27*, 19−25.

[15] S. J. Gregg, K. S. W. Sing, *Adsorption, Surface Area and Porosity*, 2nd ed., Academic Press, London, **1982**.

[16] M. Pillinger, C. D. Nunes, P. D. Vaz, A. A. Valente, I. S. Gonçalves, P. J. A. Ribeiro-Claro, J. Rocha, L. D. Carlos, F. E. Kühn, *Phys. Chem. Chem. Phys.* **2002**, *4*, 3098−3105.

[17] D. Brunel, A. Cauvel, F. Fajula, F. DiRenzo, *Zeolites: A Refined Tool for Designing Catalytic Sites* (Eds.: L. Bonneviot et al.), Elsevier Science B. V., **1995**, p. 173.

[18] A. A. Valente, I. S. Gonçalves, A. D. Lopes, J. E. Rodríguez-Borges, M. Pillinger, C. C. Romão, J. Rocha, X. García-Mera, *New J. Chem.* **2001**, *25*, 959−963.

[19] P. J. Kunkeler, J. C. Van der Waal, J. Bremmer, B. J. Zuurdeeg, R. S. Dowing, H. Van Bekkum, *Catal. Lett.* **1998**, *53*, 135−138.

[20] W. M. Carmichael, D. A. Edwards, G. W. A. Fowles, P. R. Marshall, *Inorg. Chim. Acta* **1964**, *1*, 93−96.

[21] J. M. Thomas, W. J. Thomas, *Principles and Practices of Heterogeneous Catalysis*, VCH, Weinheim, **1997**.

Received May 9, 2003

